CRYSTAL GROWTH & DESIGN

Article

Multicomponent pharmaceutical adducts of #-eprosartan: physicochemical properties and pharmacokinetics study.

Sawani G. Khare, Sunil K. Jena, Abhay T. Sangamwar, Sadhika Khullar, and Sanjay K. Mandal

Cryst. Growth Des., **Just Accepted Manuscript** • DOI: 10.1021/acs.cgd.6b01588 • Publication Date (Web): 07 Feb 2017

Multicomponent pharmaceutical adducts of α-eprosartan: physicochemical properties and pharmacokinetics study.

Sawani G. Khare[1¶], Sunil K. Jena[2¶], Abhay T. Sangamwar[3*], Sadhika Khullar[4], Sanjay K. Mandal[4]

[1]Department of Pharmacoinformatics, [2]Department of Pharmaceutical Technology (Formulations), [3]Department of Pharmaceutics, National Institute of Pharmaceutical Education and Research, Sector-67, S.A.S Nagar-160062, Punjab, India.
[4]Department of Chemical Sciences, Indian Institute of Science Education and Research Mohali, Sector-81, S.A.S. Nagar -140306, Punjab, India

[¶]These authors contributed equally to this work.

Graphical Abstract

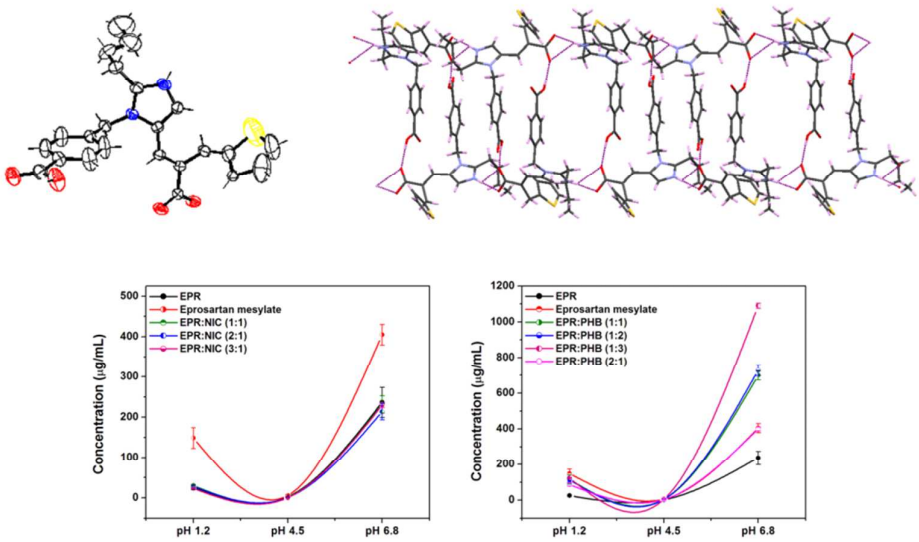

Pharmaceutical adducts of α-eprosartan (EPR) with nicotinamide (NIC) and *p*-hydroxy benzoic acid (PHB) in five different stoichiometry ratio were synthesized by liquid assisted grinding technique. The primary goal was to improve the pH dependent solubility and dissolution rate of EPR and hence its oral absorption across the gastrointestinal tract. A significant increase in oral bioavailability in overnight fasted Sprague-Dawley rats is possible with cocrystal (2.4-fold) and eutectics (6.1-fold), even when cocrystal transformation is suspected based on *in vitro* studies.

[*]Corresponding author
Abhay T. Sangamwar, Ph.D
Assistant Professor, Department of Pharmaceutics
National Institute of Pharmaceutical Education and Research, S.A.S Nagar, Punjab-160062, India
Tel: +91-0172 2214682; Fax: +91-0172 2214692
E-mail: abhays@niper.ac.in, abhaysangamwar@gmail.com

Title

Multicomponent pharmaceutical adducts of α-eprosartan: physicochemical properties and pharmacokinetics study.

Author names and affiliations

Sawani G. Khare[1¶], Sunil K. Jena[2¶], Abhay T. Sangamwar[3*], Sadhika Khullar[4], Sanjay K. Mandal[4]

[1]Department of Pharmacoinformatics, National Institute of Pharmaceutical Education and Research, Sector-67, S.A.S Nagar-160062, Punjab, India.

[2] Department of Pharmaceutical Technology (Formulations), National Institute of Pharmaceutical Education and Research, Sector-67, S.A.S Nagar-160062, Punjab, India.

[3] Department of Pharmaceutics, National Institute of Pharmaceutical Education and Research, Sector-67, S.A.S Nagar-160062, Punjab, India.

[4] Department of Chemical Sciences, Indian Institute of Science Education and Research Mohali, Sector-81, S.A.S. Nagar -140306, Punjab, India

[¶]These authors contributed equally to this work.

[*]Corresponding author

Abhay T. Sangamwar, Ph.D
E-mail: abhays@niper.ac.in, abhaysangamwar@gmail.com

Abstract

Pharmaceutical adducts of α-eprosartan (EPR) with nicotinamide (NIC) and *p*-hydroxy benzoic acid (PHB) were prepared by liquid assisted grinding technique. Prior to conducting this study, the crystal structure of EPR was determined. This study was designed to improve the pH dependent solubility and dissolution rate of EPR and hence its oral absorption across the gastrointestinal tract. Initially, differential scanning calorimetry (DSC) and powder X-ray diffractometry (PXRD) were used as a screening tool for rapid cocrystal or eutectic mixture screening. The eutectic mixture of EPR with PHB in 1:3 stoichiometry ratio show better

solubility and dissolution rate in all aqueous buffer as compared to EPR:NIC cocrystals and EPR. EPR:NIC cocrystal in 1:1 stoichiometry ratio show better dissolution rate initially as compared to pure EPR but does revert back to EPR within the first 30 min in pH 1.2 and 6.8. Absorption and desorption profile of EPR adducts are reversible suggesting no solid state transformation under experimental conditions. A significant increase in oral bioavailability in over night fasted Sprague-Dawley rats is acheived with cocrystal (2.4-fold) and eutectics (6.1-fold), even when cocrystal transformation is suspected based on *in vitro* studies.

Key words

Eprosartan, Cocrystals, Eutectics, Solubility, Dissolution rate, Bioavailability

Introduction

Nearly, 70-80% of new drug candidates in the development pipeline are poorly water soluble. The problem of poor solubility became more pervasive with high-throughput screening (HTS) methodology. HTS methodology utilize advances in genomics and combinatorial chemistry for lead identification in drug discovery. The poor water solubility attributed to the presence of polycyclic rings, rendering them more lipophilic for accessing the molecular target located inside the cell[1]. However, the limited dissolution rate arising from poor aqueous solubility results in low oral bioavailability, thus limiting drug concentration at the target site[2]. According to the US Food and Drug Administration (FDA), drug candidates with low solubility and high permeability are classified as Biopharmaceutics Classification System (BCS) class II[3]. Increasing the aqueous solubility and thus bioavailability of such drugs is currently one of the main challenges in pharmaceutical industry. Various formulation strategies commonly employed for improving the solubility of

drugs include salt formation[4], micronization[5], nanocrystals[6], self-emulsification system[7], amorphous solid dispersion[8], co-crystal[9], phopholipid-drug complex[10] and cyclodextrin complexation[11]. Perhaps, the salt formation for drugs with an ionizable center is the most obvious and easy approach for improving the solubility. However, non-toxic counter ions for salt formation are limited[12]. In recent years, cocrystal approach is extensively used to improve the solubility of drug[9]. Additionally, cocrystal form do not alter the basic molecular structure of an active pharmaceutical ingredient (API). Furthermore, rearrangement of molecular packing in the crystal lattice may improve the physicochemical properties of the drug[13]. Pharmaceutical cocrystal is defined as a crystalline molecular complex that contain one of the components as an API and another component called coformer. The two different molecules (i.e., drug and coformer) are arranged in the crystal lattice through hydrogen bonding[14], van der Waals forces[15], metal co-ordination[16], π-π stacking[17] and electrostatic interactions[18]. However, during co-crystallization several API form eutectic mixtures instead of cocrystals[19].

Rational designing of pharmaceutical cocrystals with enhanced physicochemical properties can be achieved by applying crystal engineering approaches, which exploits the knowledge of intermolecular interactions in crystal packing. These non-covalent interactions trigger the formation of supramolecular synthons[20]. Supramolecular synthons can be classified into two categories *viz.* homosynthons and heterosynthons. The supramolecular homosynthons can be formed in a single component compounds, whereas supramolecular heterosynthon is formed between two functional groups that are located on different molecules which lead to the formation of a multi-component crystals. Hence, heterosynthons

are more amenable to form cocrystals. The most critical step in the cocrystal formation is the selection of coformer. Supramolecular synthon corroborate the way of conformer screening which utilizes the data from Cambridge Structural Database (CSD).

Eprosartan, chemically known as 4-({2-Butyl-5-[2-carboxy-2-(thiophen-2-ylmethyl)eth-1-en-1-yl]-1*H*-imidazol-1-yl}methyl)benzoic acid is an angiotensin II receptor antagonist, innovative by Kos Life Sciences, Inc. and prescribed for the treatment of high blood pressure and also rarely used as a second line therapy for congestive heart failure[21]. The eprosartan exists as a salt form and marketed as solid unit dose which consists of 80%, by weight, amorphous eprosartan mesylate[22]. Based on its aqueous solubility (~8.33 μg/mL), it is classified as a BCS class II drug, pH dependent aqueous solubility further limits its oral absorption and bioavailability (~15%)[23]. Formulation approaches including nanocrystal[24], amorphous solid dispersion[22], and immediate release tablets[25] have been attempted more precisely to improve the aqueous solubility of eprosartan. Recently, eprosartan cocrystals are reported in improving the solubility and dissolution rate of eprosartan[26]. However, the pH effect on cocrystal solubility has not been established. pH-dependent aqueous solubility of eprosartan is one of the determining factors which limits its oral absorption and bioavailability[27] therefore, a correlation between the pH dependent solubility of α-eprosartan cocrystals and its subsequent effect on oral bioavailability will further establish the efficacy of cocrystals.

In this study, we investigated the solubility and dissolution profile of three cocrystals and four eutectics of α-eprosartan (EPR) at different physiological conditions and compared it with its salt form (i.e. eprosartan mesylate). Moreover, the pharmacokinetic study of

EPR:NIC (1:1) co-crystal and EPR:PHB (1:3) eutectic mixture (selected due to improved physicochemical properties) were performed in Sprague-Dawley rats and compared with eprosartan mesylate.

Experimental Section

Materials

Eprosartan mesylate was generously provided by Glenmark Pharmaceuticals Ltd. (Mumbai, India) as a gift sample and used as a source to obtain free acid eprosartan and EPR. Nicotinamide (NIC) was purchased from Sigma-Aldrich (Bangalore, India). p-hydroxybenzoic acid (PHB) was purchased from HiMedia Laboratories (Mumbai, India). Acetone LR grade was purchased from Merck Specialities Pvt. Ltd. (Mumbai, India). Ethanol absolute AR grade was purchased from Changshu Yangyuan Chemical Co., Ltd. (Jiangsu, China). All other chemicals and reagents were of analytical or chromatographic grade and used without further purification.

Preparation of eprosartan free acid from eprosartan mesylate

Eprosartan free acid was prepared according to the method as adopted by Link et al.[28] with slight modification. Briefly, 5 g of eprosartan mesylate was suspended in 100 mL of distilled water under stirring at room temperature and adjusting the pH of the resultant suspension to about 2.0 with 1.0 N HCl. The precipitated eprosartan free acid was collected by filtration and air dried. The crude eprosartan free acid was further purified by dissolving it in small amount of methanol at room temperature, filtered and recrystallized at 4ºC using water and ethyl acetate as a solvent system. [% Yield: 68%; Melting point: 226.41ºC]

Preparation of eprosartan form-α (EPR)

Polymorphic form-α of eprosartan was synthesized according to the method as adopted by Link et al.[28] with slight modification. Briefly, accurately weighed 1 g of eprosartan was dissolved in 20 mL of acetic acid by heating to 110ºC. The solution was allowed to cool at room temperature; during this cooling, at 60ºC methanol ~ 40 mL was added slowly. The resultant mixture was aged at 2-8ºC for 24 h. The product was filtered and vacuum dried at 45ºC. [% yield: 85%; Melting point: 267.5ºC].

Preparation of cocrystals/eutectic mixtures

Cocrystals of EPR were obtained by liquid-assisted grinding technique. Two potential coformers at five different molar ratio (i.e. 1:1, 1:2, 1:3, 2:1 and 3:1) with respect to EPR were evaluated for successful cocrystal/eutectic formation.

Around 100 mg of EPR:NIC cocrystals or eutectic mixtures were obtained upon grinding different molar ratio of EPR and NIC for 30 min by ethanol liquid-assisted grinding. The powder so obtained was vacuum dried at 40°C for 24 h and used as such for solid state characterization. Similarly, EPR:PHB cocrystals or eutectic mixtures were prepared. All the preparations were passed through 40 mesh screen and then stored at room temperature until further used. Efforts have been made to prepare the quality single crystals of EPR:NIC and EPR:PHB, but remained unsuccessful.

Characterization of eprosartan free acid

Electrospray ionization-mass spectroscopy measurement of eprosartan free acid and eprosartan mesylate was performed using MAT LCQ mass spectrometer (Thermo Finnigan, California, U.S.A) equipped with electrospray ionization (ESI) probe and an atmospheric pressure chemical ionization (APCI) probe. The mass spectrometer and all peripheral

components were controlled through the Finnigan Xcalibur software v 1.3.

Characterization of EPR

Differential scanning calorimetry: Differential scanning calorimetry (DSC) measurement of eprosartan mesylate, eprosaratn free acid and EPR was performed using Q2000 (TA Instruments, Delaware, U.S.A) equipped with Universal® analysis 2000, version 4.5 A software. Each sample was carefully weighed in a crimped aluminum pan with a pierced lid. The samples were scanned from 25-350ºC at a heating rate of 10ºC/min in an atmosphere of nitrogen gas. The DSC was calibrated for baseline using empty pans, and for temperature and enthalpy with indium.

Powder X-ray diffraction: Powder X-ray diffraction measurement of eprosartan mesylate, eprosartan free acid and EPR was recorded at room temperature on a Bruker's D8 Advance X-ray diffractometer (Karlsruhe, Germany) using Cu-Kα radiation as X-ray source (λ = 1.54 Å) at 35 kV, 30 mA passing through a nickel filter. Data was collected in a continuous scan mode (2θ min^{-1}) with a step size of 0.01 s and step time of 1 s over an angular range of 4 to 40° in 2θ.

Single crystal X-ray diffraction: Single crystals of EPR were grown in absolute ethanol. Initially, 50 mg of EPR was added to 4 mL of absolute ethanol and the glass vial was heated to dissolve the content. The vial was sealed and allowed to cool slowly overnight at room temperature. The resulting crystals of EPR was isolated and crystal structure was examined. Initial crystal evaluation and data collection was performed on a Kappa APEX II diffractometer equipped with a CCD detector (with the crystal-to-detector distance fixed at 60 mm) and sealed-tube monochromated MoK α radiation using the program APEX2[29]. By

using the program SAINT[29] for the integration of the data, reflection profiles were fitted, and values of F^2 and $\sigma(F^2)$ for each reflection were obtained. Lorentz and polarization effects were used for the data correction The subroutine XPREP[29] was used for the processing of data that included determination of space group, application of an absorption correction (SADABS)[29], merging of data, and generation of files necessary for solution and refinement. The crystal structure was solved and refined using SHELX 97[30]. Based on systematic absences, the space group was chosen and confirmed by the successful refinement of the structure. Positions of most of the non-hydrogen atoms were obtained from a direct methods solution. Several full-matrix least-squares/difference Fourier cycles were performed, locating the remainder of the non-hydrogen atoms. A lot of effort was put to model the disorded thiophene ring but only the sulfur atom could be put into two different positions with equal occupancy in obtaining reasonable metric parameters, thermal parameters and converged refinement. Furthermore, an appropriate DFIX command was used to make the bond distances acceptable for the structure. The use of SQUEEZE program did not improve the situation for R-factors. All non-hydrogen atoms except one of carbon atoms in the thiophene ring (C22) and the solvent molecule were refined with anisotropic displacement parameters. All hydrogen atoms except C23 attached to the disordered sulfur atom were placed in ideal positions and refined as riding atoms with individual isotropic displacement parameters. All figures were drawn using MERCURY V 3.0[31] and Platon[32].

Solid state characterization of cocrystals/eutectic mixtures

Differential Scanning Calorimetry(DSC): Recently, Lu et al.demonstrate that DSC could be used as an efficient and rapid cocrystal screening tool[33]. Thus, DSC method was adopted to

screen the possible cocrystal or eutectic mixtureformation of EPR with two different coformers. The DSC measurements of EPR, coformers and prepared cocrystals or eutectic mixtures were performed as per the method as described above.

Powder X-Ray Diffraction (PXRD):The PXRD pattern of a crystalline sample is considered as the fingerprint of its crystal structure. Every new crystalline material exhibit unique peak indicative of reflections from specific atomic planes, giving rise to the unique pattern. PXRD measurement of pure drug eprosartan mesylate, EPR, coformers and possible EPR cocrystals or eutectic mixtures were performed as per the methodology as described above.

pH dependent solubility measurement

Saturation solubility measurement of eprosartan mesylate, EPR, and possible EPR cocrystals or eutectic mixtures were performed in 0.1 N HCl (pH 1.2), phthalate buffer (pH 4.5) and phosphate buffer (pH 6.8). Briefly, excess quantity of each sample was suspended in 5 mL aqueous solutions of different pH in sealed glass vials. The vials were agitated at 100 rpm for 72 h in the shaker water bath (EQUITRON®, Medica Instrument Mfg. Co., India) maintained at 37 ± 0.5ºC. The dispersion was centrifuged (OptimaTM LE-80K, Beckman Coulter, USA) at 10,000 rpm for 10 minutes at 4ºC. The supernatant was filtered through 0.45 µm PVDF syringe filter, Millipore Millex-HV and suitably diluted with methanol before analysis. Each experiment was performed in triplicate.

Reverse phase high performance liquid chromatography (HPLC) method was used for the quantification of EPR in all samples. HPLC system was comprised of a Waters 2695 separation module equipped with a quaternary pump, an auto sampler unit, and a Waters 2996 photodiode array (PDA) detector. Agilent's ZORBAX Eclipse XDB-C18 analytical column

(5µm; 4.6 × 150 mm) (Agilent Technologies, Inc. USA) was used for the estimation of EPR. Methanol and phosphate buffer (10 mM, pH 3.0) in 60:40 (% v/v) proportions were used as a eluent for the estimation of EPR. The flow rate was maintained at 0.6 mL/min and EPR was detected at 232 nm using a PDA detector. The Empower HPLC software was used for the analysis of data.The method was found to be linear in the working range of 2.5-15.0 µg/mL (co-efficient of regression, r^2 = 0.998). The limit of detection (LOD) and limit of quantification (LOQ) were 0.80 and 2.43 µg/mL, respectively. A 10µL of the supernatant was injected into the HPLC system.

***In vitro* drug release experiment**

Dissolution rate measurements of eprosartan mesylate, EPR, and possible EPR cocrystals or eutectic mixtures were performed in USP 37 type II automated dissolution test apparatus (ElectrolabTDT-08L, Mumbai, India) in three different buffers (i.e. 0.1 N HCl, pH 1.2; phthalate buffer, pH 4.5; and phosphate buffer, pH 6.8). Each samples, equivalent to 100 mg of EPR, were placed in the dissolution vessel containing 900 mL buffer previously maintained at 37 ± 0.5°C and stirred at 50 rpm. Aliquots of sample were collected at different time intervals and replaced with a fresh dissolution medium to maintain the sink condition. The samples were centrifuged (Optima™ LE-80K, Beckman Coulter, USA) at 10,000 rpm for 10 min at 4 ºC and filtered through 0.45 µm PVDF syringe filter, Millipore Millex-HV to remove the undissolved drug. Each experiment was performed in triplicate.

Dynamic Vapor Sorption

Dynamic vapor sorption (DVS) studies for pure drug eprosartan mesylate, EPR, EPR:NIC (1:1) co-crystal and EPR:PHB (1:3) eutectic mixture were performed using DVS,

Model Q5000 SA (TA Instruments, Delaware, U.S.A) to understand the hygroscopic nature of solids. Briefly, each sample was weighed and transferred to the tared sample pan. Samples were equilibrated at 25°C for 60 min and vapor sorption isotherms were measured by increasing relative humidity from 0 to 90% using nitrogen environment at 10% step size.

In-vivo oral pharmacokinetics study

Animals: Female Sprague-Dawley rats weighing 180-200 g, 6-7 weeks old were obtained from the central animal facility (CAF), National Institute of Pharmaceutical Education and Research (NIPER), S.A.S Nagar, India. The animals were housed at 22 ± 2°C and 50-60% relative humidity (RH) under 12h light/dark conditions for one week before the commencement of experiment. Standard pellet diet (Ashirwad Industries, Kharar, Punjab, India) and water was given *ad libitum.* The study protocol was duly approved by the Institutional Animal Ethics Committee (IAEC), NIPER, S.A.S Nagar, India (IAEC/15/15; 24th April, 2015).

Pharmacokinetics study: Twenty animals were randomly distributed into four groups, each containing five animals, as described below. Before the commencement of study, animals of each groups were fasted overnight with free access to water for 12 h.

Group I: Administered EPR suspension in double distilled water containing 0.2% w/v sodium carboxymethylcellulose as suspending agent, at a dose equivalent to 40 mg/kg body weight EPR, peroral (p.o.).

Group II: Administered eprosartan mesylate suspension in double distilled water containing 0.2% w/v sodium carboxymethylcellulose as suspending agent, at a dose equivalent to 40 mg/kg body weight of eprosartan, p.o.

Group III: Administered EPR:NIC cocrystal (1:1) suspension in double distilled water containing 0.2% w/v sodium carboxymethylcellulose as suspending agent, at a dose equivalent to 40 mg/kg body weight of eprosartan, p.o.

Group IV: Administered EPR:PHB eutectic mixture (1:3) suspension in double distilled water containing 0.2% w/v sodium carboxymethylcellulose as suspending agent, at a dose equivalent to 40 mg/kg body weight of eprosartan, p.o.

Retro-orbital plexus was selected for the collection of blood samples under mild anesthesia. The blood samples were collected into the micro centrifuge tubes containing heparinized saline (40 IU/mL blood) at 0.5, 1, 2, 4, 6, 8, 12 and 24 h. Blood samples were centrifuged at10,000 rpm for 10 min at 4°C and stored at -20°C prior to analysis.

Quantification of EPR in plasma samples: EPR quantification in plasma samples were carried out by the reverse phase HPLC method as adopted by Jena et al.[10,34] with slight modification. Briefly, a 0.1 mL aliquot of plasma sample was mixed with 50 µL methanol containing internal standard (IS) naproxen 50 µg/mL and vortexed for 30 Sec. A 200 µL volume of mixture of methanol and acetonitrile in 1:1 proportion as extraction solvent was added and vortexed for another 3 min. The mixture was centrifuged at 10,000 rpm for 10 min at 4°C and the supernatant was filtered through 0.45 µm PVDF syringe filter, Millipore Millex-HV. The filtrate (10 µL) was injected into the HPLC system for the detection of EPR. Agilent's ZORBAX Eclipse XDB-C18 (5 mm; 4.6 × 150 mm) analytical column was used for the separation of EPR in plasma samples. Methanol and phosphate buffer (10 mM, pH 3.0) in 61:39 proportions were used as an eluting agent. The flow rate was adjusted at 0.8 mL/min, the run time was 16 min and injection volume was 50 µL. EPR was quantified using a PDA

detector at 232 nm. Kinetica software version 5.0 (Thermo Fisher Scientific Inc., USA) was used to calculate the pharmacokinetic parameters.

Statistical data analysis

The mean and standard deviation (SD) of all values were calculated. The statistical comparisons were performed by one-way analysis of variance (ANOVA) using GraphPad Prism 5 software, version 5.04 (GraphPad Software, Inc San Diego, CA, USA). The results were considered statistically significant when $p < 0.05$.

Results and discussion

Characterization of eprosartan free acid

Eprosartan free acid was successfully prepared and recrystallized. Electrospray ionization (ESI) mass spectrum of eprosartan (**Figure S1**) shows abundant $[M]^+$ (*m/z* 424.98) ions, corresponding the molecular weight of eprosartan free acid. DSC thermogram of eprosartan mesylate (**Figure S2**) exhibits a sharp endothermic peak at 251.67°C corresponding to phase transition temperature. However, eprosartan free acid exhibits two endothermic peaks; the first broad peak appears at 226.41°C and another at 228.95°C, both peaks are overlapped suggesting a reversible endothermic transition of one polymorphic form into another polymorphic form at 210-240ºC. Moreover, the appearance of new peaks in X-ray powder diffractometry of eprosartan free acid as compared with pure eprosartan mesylate clearly indicates the formation of new crystalline solid phases (**Figure S3**).

Characterization of EPR

Polymorphs of an API exhibit different chemical and physical properties which have a greater impact on process-ability of API and quality/performance of the fished product in

terms of stability, dissolution and bioavailability. Hence, selection of a specific polymorph of an API is important. Generally, metastable forms are more soluble than their corresponding stable polymorphic forms, but they transform to the more thermodynamically stable form in a relatively short time[35], and thus it is necessary to monitor the polymorphic transformation during formulation, manufacturing, and storage of dosage forms to ensure reproducible bioavailability after administration[36]. The single and sharp endotherm at around 267.49ºC corresponds to the melting curve of EPR[28]. **Figure S3** illustrates the PXRD patterns of eprosartan free acid and EPR. As can be seen, EPR exhibits clearly distinct peaks as compared to eprosartan free acid and the position of the peaks are found to be in good agreement with the reported work[28]. Schematic views of EPR are illustrated in **Figure S4**. The crystallographic data and hydrogen bonding parameters of EPR crystal are presented in **Table S1 and S2,** respectively. In the α-form, the asymmetric unit consist of only one molecule of EPR in which free eprosartan exists as a zwitterion where the proton from the aliphatic carboxylic acid group is transferred to the imidazole nitrogen. Further, the two molecules of EPR are held together through O-H…O hydrogen bonding (O2-H17…O5, distance (O2...O5): 2.561 Å and angle 173.8^{o}) to form dimers (**Figure S5**) where the carbonyl proton on one molecule serve as donor and the deprotonated carbonyl group on another as acceptor. In addition, these two asymmetric units are packed together in pairs through N-H…O hydrogen bonding (N2-H3…O4, 2.670 Å; N2-H3, 0.86 Å; H3…O4, 1.81 Å; N2-H3…O5, 3.175 Å; N2-H3, 0.86 Å; H3…O5, 2.59 Å) where the proton from imidazole nitrogen serve as donor and the carbonyl oxygen in another serve as acceptor. Again, these tetramers are packed together in pairs through same set of N-H…O hydrogen bonding

between the imidazole nitrogen of one tetramer serving as proton donor and the carbonyl oxygen in another tetramer serving as acceptor (**Figure S6**).

Solid state characterization of cocrystals/eutectic mixtures

Differential Scanning Calorimetry: Examination of the crystal structure of EPR reveals that the carboxylic acid and imidazole group are the main proton acceptor and donor group for H-bond formation in supramolecular synthons. Hence, two USFDA-approved coformers (NIC and PHB) with complementary functional groups i.e. amide and carboxylic acid were selected for the cocrystallization experiments. Ten binary systems with two different coformers in different stoichiometry were checked by DSC for cocrystal formation with EPR. Three new cocrystals and four eutectic mixtures were obtained. Recently, Lu et al. demonstrate that DSC could be used as an efficient and rapid cocrystal screening tool[33]. To apply this method, two individual components were mixed and ground by liquid-assisted grinding technique in different stoichiometric proportions and placed in crucibles. There were distinctive melting peaks on the DSC curve, which were later analyzed to identify the cocrystal and eutectic mixture using the rules suggested by Lu et al.[37]and Yamashita et al.[38]. According to these rules, mixture of individual components are capable of forming cocrystals if the following conditions are fulfilled: (a) the physical mixturemelting produces two peaks corresponding to eutectic mixture and cocrystal melting (with their temperatures being different from the melting temperatures of individual components)[37], (b) the eutectic melting (the first peak) is followed by a small exo-effect[38].

Table 1 summarizes the obtained DSC results for different mixtures tested. Among all the mixture screened, only three showed a positive result for cocrystal formation. It is

northeworthy to note that sharp melting peak at around 188.9ºC and 175.4ºC was observed in case of the EPR:NIC (1:1) and (2:1), respectively. Moreover, this melting endotherm lies in the region between the melting points of individual components, EPR (267.5ºC) and nicotinamide (130.3ºC) and hence clearly indicates the formation of new crystalline phase. However, an exo-effect at 176.2ºC was clearly seen before melting endotherm at 189.5ºC in EPR:NIC (3:1) indicating cocrystal formation (**Figure 1**).The appearance of first peak in all the binary mixtures corresponds to the fusion of coformers with EPR forming eutectic mixtures, while the second peak corresponds to the melting of either cocrystal or excessive amount of the component with higher melting point[39]. Manin et al. revealed that if the melting temperatures difference is over 50ºC for the pure individual components and one endothermic peak of the physical mixture appeared below the melting temperature of the more volatile component, then definitely no cocrystal was formed in the system[40].Based on this theory, only three cocrystals were formed out of 10 systems and rest of them forms eutectic mixtures. Moreover, the absence of second event in all the binary mixtures of EPR with PHB (**Figure 2**) confirms the formation of eutectic mixtures. The first, second and third broad melting endotherms in EPR:NIC (1:2) and (1:3) corresponds to the melting of eutectic mixture formed by the fusion of NIC with EPR, cocrystal and excessive amount of individual components, respectively.The possible cocrystal and eutectic mixtures were further analyzed by PXRD.

Table 1 The melting endotherms and exotherms of ground mixture of EPR with NIC and PHB.

Coformers	**Molar ratio (EPR:coformer)**	**Endotherm (°C)**		**Exothermic peak (Yes/No) (°C)**	**Cocrystal /Eutectic mixture**
		1st peak	**2nd peak**		
NIC	1:1	95.5	188.9	No	Cocrystal
	1:2	103.5	133.1	No	Eutectic mixture
	1:3	98.7	134.7	No	Eutectic mixture
	2:1	81.4	175.4	No	Cocrystal

	3:1	172.5	189.5	Yes, 176.2	Cocrystal
PHB	1:1	170.0	-	No	Eutectic mixture
	1:2	169.3	-	No	Eutectic mixture
	1:3	171.9	201.1	No	Eutectic mixture
	2:1	167.4	232.9	No	Eutectic mixture
	3:1†	-	-	-	-

† Sticky product

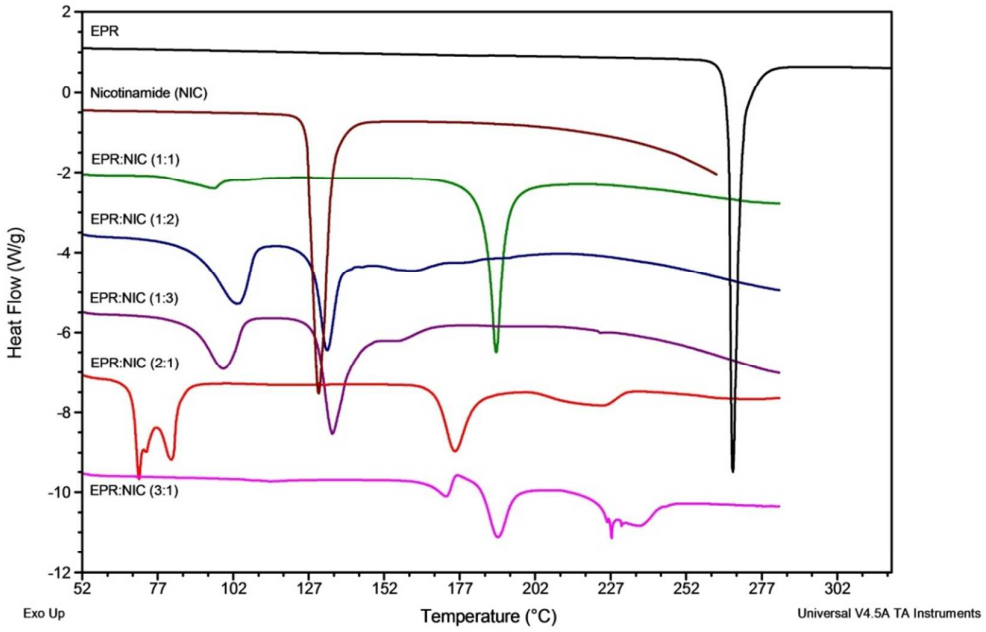

Figure 1. DSC thermograms of solid ground mixture of EPR with NIC in different stoichiometric ratio.

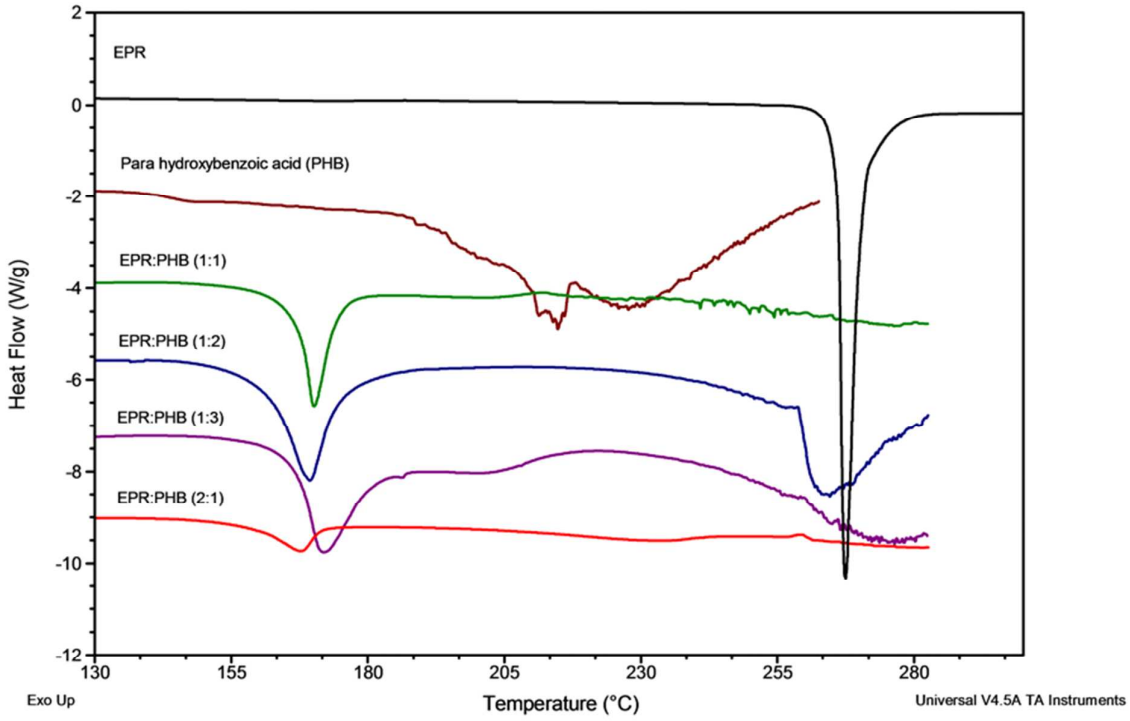

Figure 2. DSC thermograms of solid ground mixture of EPR with PHB in different stoichiometric ratio.

Powder X-Ray Diffraction (PXRD): **Figure 3** and **4** illustrates the PXRD patterns of possible EPR cocrystals with nicotinamide and eutectic mixtures with PHB, respectively as confirmed previously by DSC. Analysis of diffraction patterns of EPR:NIC (1:1, 2:1 and 3:1) has shown a distinct crystalline phase with a considerable difference in [*d*] spacing values from that seen with either of the individual components suggesting the formation of new phase as marked by asterisks. On the contrary, the characteristic reflections of EPR and PHB were retained in all the binary mixtures of EPR with PHB, and shows no significant difference in [*d*] spacing values from that seen with either of the individual components. Also, the relative intensities of the observed reflections vary gradually with mass fractions. These results signify that liquid assisted grinding results in microcrystalline powders where either two crystalline components are phase separated[41] and/or one component might present as ultrafine crystals in

the second major component usually polymer or coformers[42,43]. The present PXRD results are in good agreement with the DSC results mentioned above. Thus, PXRD along with DSC presents an effective method for the rapid screening of cocrystals.

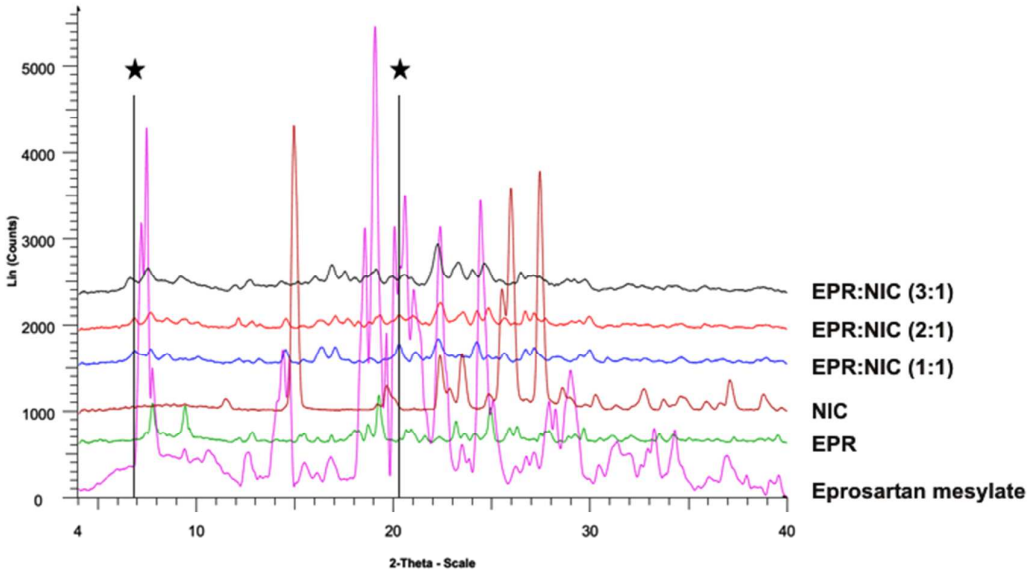

Figure 3. PXRD patterns of cocrystals of EPR with NIC in different propotions.

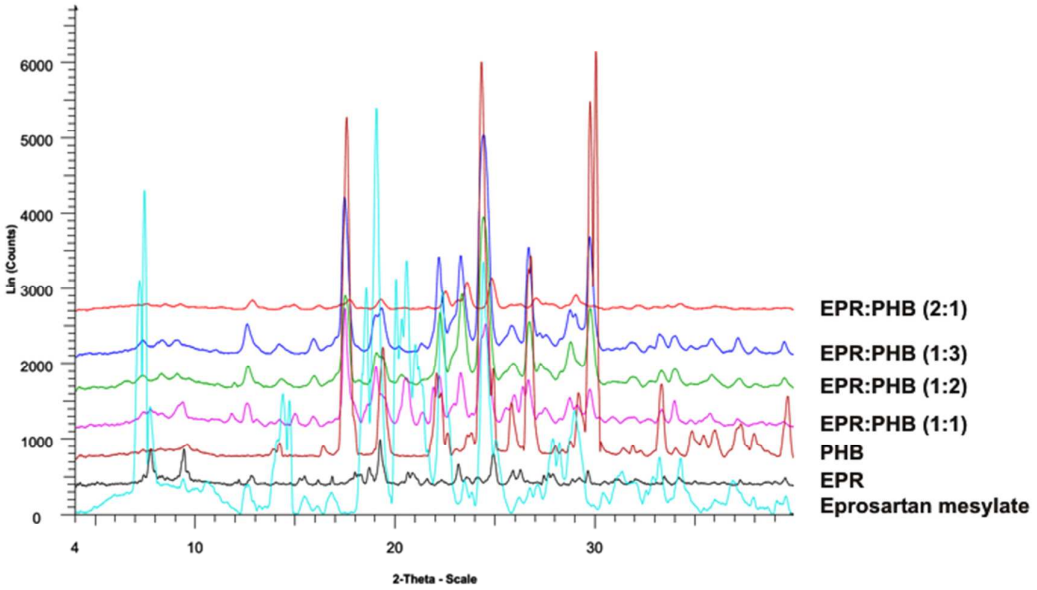

Figure 4. PXRD patterns of eutectic mixtures of EPR with PHB in different propotions.

pH dependent solubility measurement

The results of solubility experiment are illustrated in **Figure 5**. As can be seen, eutectic mixtures exhibits higher solubility than their counterpart cocrystals in 0.1 N HCl, pH 1.2. In addition, eutectic mixtures are more soluble than the EPR and cocrystals in phthalate (pH 4.5) and phosphate (pH 6.8) buffer, also. This increase in apparent solubility in eutectics attributed to the presence of weaker intermolecular interactions and high surface free energy[39]. Moreover, all the preparation exhibits pH dependent solubility. Like, in case of EPR the solubility was maximum (236.74 ± 37.31 μg/mL) at pH ≥ 6.8, but has a solubility of 25.36 ± 5.27 μg/mL at pH ≤ 1.2, its solubility decreased by about 10-fold with constant low solubility value of around 2.51 ± 0.12 μg/mL at pH equal to 4.5. A similar pattern were observed between the solubility of EPR and cocrystals in all the aqueous buffer studied. Interestingly, the same solubility pattern was observed with eutectics and eprosartan mesylate. This pH dependent solubility was expected considering the pKa value of coformers (nicotinamide, pKa ~ 3.35 to 3.43 and PHB, pKa ~ 4.48)[44,45] and EPR (pK_1 ~ 3.63 and pK_2 ~ 6.93)[46]. It has been assumed that cocrystals remains stable at pH 3.0 to 3.5 but transform to individual components at pH ≤ 2.0 and pH ≥ 4. This means that cocrystals will have a solubility of either EPR or NIC at pH 3.0 to 3.5, while more soluble at pH ≤ 2.0 and pH ≥ 4. Conversely, there was no significant difference between the solubility of cocrystals and EPR in all aqueous buffer. This might be due to the nonavailability of excess amount of coformer NIC to maintain the thermodynamic stability of EPR:NIC cocrystal in aqueous solution. It has been reported that as cocrystal solubility increases above the drug solubility, higher coformer concentrations are needed to maintain cocrystal stability[47]. On the contrary, large excess of

PHB in aqueous buffer stabilizes the interaction between the EPR and PHB in solution state and hence increases the apparent solubility of EPR at pH 1.2 and 6.8.

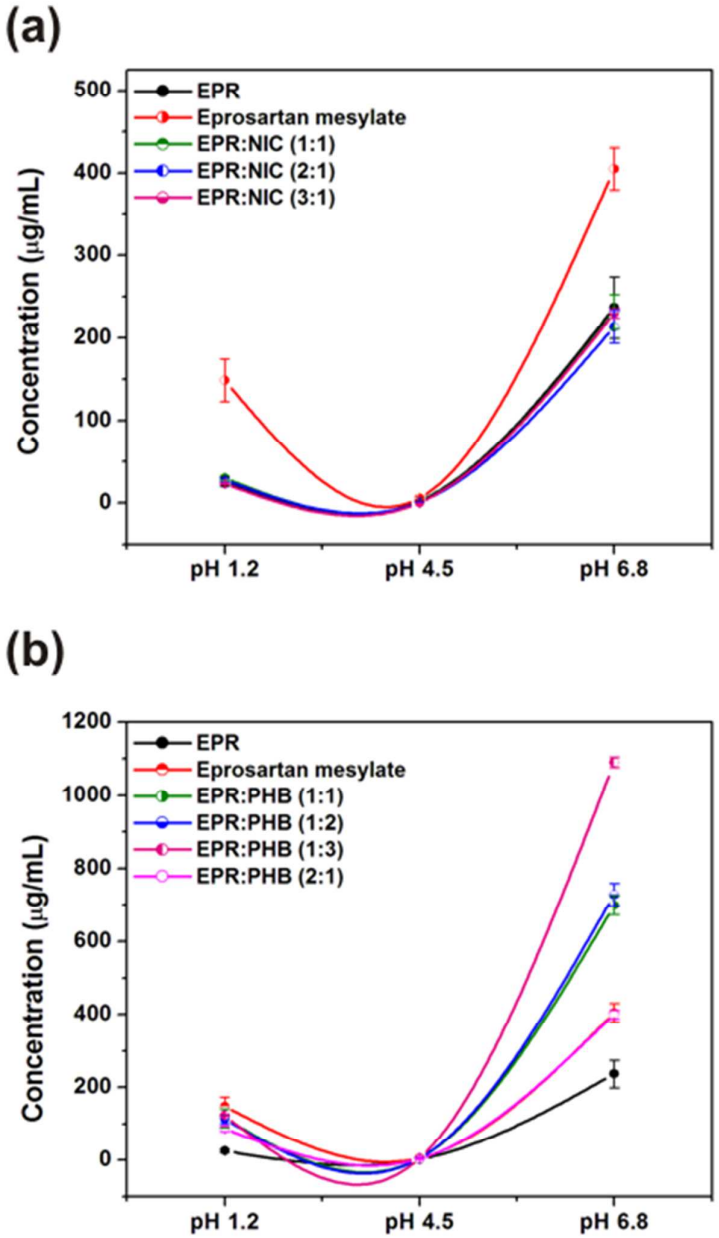

Figure 5. Solubility profile of **(a)** EPR cocrystals with NIC and **(b)** EPR eutectic mixtures with PHB at different pH conditions.

Dissolution experiment

Figure 6 illustrates the dissolution profile of EPR, eprosartan mesylate and EPR-cocrystals or eutectic mixtures in three different media (i.e. 0.1 N HCl, pH 1.2;

phthalate buffer, pH 4.5; and phosphate buffer, pH 6.8). As can be seen, EPR release from EPR-cocrystals or eutectic mixtures were affected by the pH of the dissolution media. EPR being zwitteronic in nature has exhibited pH dependent solubility. The increase in dissolution rate is particularly important considering the pKa of EPR ~ 3.63 and 6.93. Maximum absorption occurs below this pH. Enhancement of dissolution rate in the acidic pH, thus has the potential to increase its bioavailability. The dissolution rate was significantly enhanced ($p < 0.05$) in 0.1 N HCl, pH 1.2 with EPR:NIC cocrystals releasing 35.26 ± 2.36, 21.47 ± 1.42 and 15.47 ± 1.71% EPR from EPR:NIC (1:1), (2:1) and (3:1), respectively within first 30 min as compared to pure EPR alone which exhibited a dissolution of 3.24 ± 2.26% at the same time point. However, the transformation of EPR:NIC cocrystals to individual component was observed within 30 min in 0.1 N HCl aqueous media, pH 1.2[47]. An initial enhancenment in dissolution rate was observed and thereafter maintenance of cocrystal form resulted in rapid dissolution before transformation to the original EPR[48]. In contrast, EPR:PHB eutectic mixtures exhibit better dissolution profile as compared to cocrystals, releasing more than 44% EPR within the same time point. The possible mechanism for this enhanced dissolution rate from eutectic mixtures was attributed to the immediate release of ultrafine crystals into the dissolution media. Eutectics are known to have better dissolution profile as compared to their cocrystal counterparts due to the presence of high surface free energy, molecular mobility and weak intermolecular interactions[39]. Moreover, the excess of coformer in solution prevents the dissociation of EPR:PHB eutectic mixtures. This phenomenon might be associated with eutectic constants (K_{eu}), a factor that determines the solubility and thermodynamic stability of cocrystals or eutectic mixtures in aqueous solution[49]. Conversely, the cocrystals remained

stable at pH 4.5 and exhibited dissolution profile as similar to pure drug EPR releasing only 1.54 ± 0.11, 1.07 ± 0.13 and 1.14 ± 0.12% EPR within the first 30 min as compared to pure drug EPR which release 1.43 ± 0.12% drug in the same time point. However, a significant rise and rapid decline in dissolution rate from EPR:NIC cocrystals at pH 6.8 attributable primary to the pK_a value of nicotinamide (pK_a ~ 3.47). At pH ≤ 3.0 and pH ≥ 6.0, the cocrystals dissociate into their individual components and shows solubility of either of the individual components, while it remains stable between pH 3.0 and 6.0. Eutectics are more soluble and stable at both pH 4.5 and 6.8. The increased dissolution rate is attributable to the presence of ultrafine crystals in the eutectic samples.

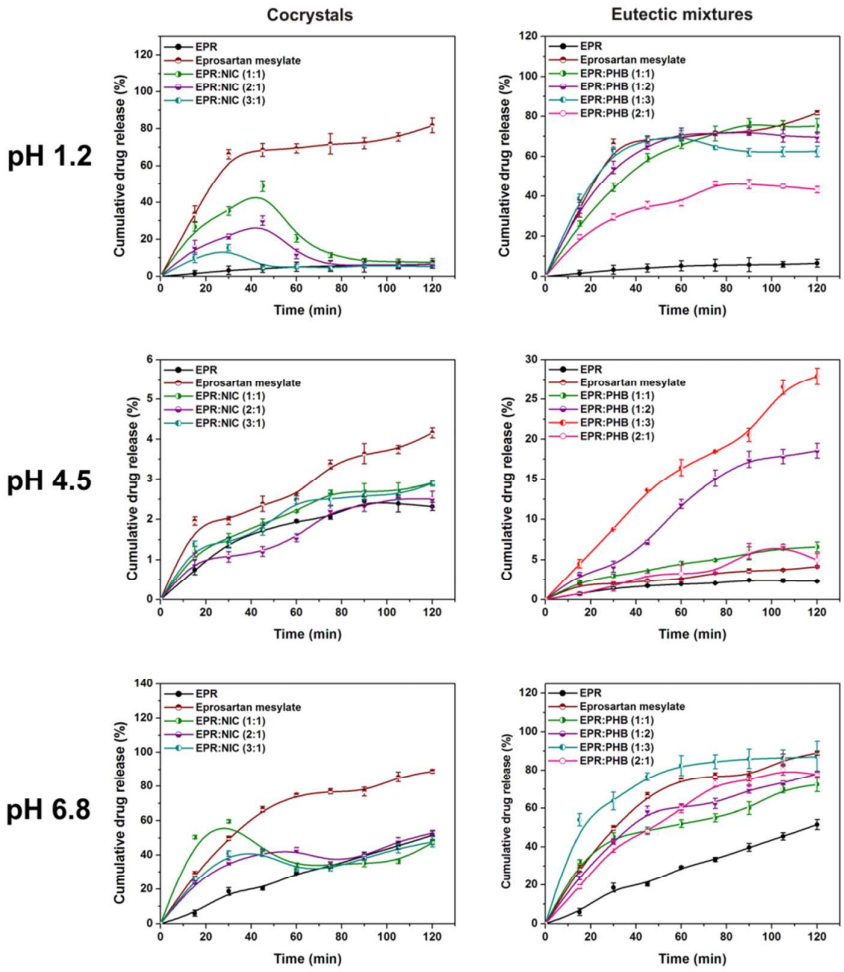

Figure 6. Dissolution profiles of EPR cocrystals with NIC and EPR eutectic mixture with PHB at pH 1.2, 4.5, and 6.8.

Dynamic Vapor Sorption (DVS)

Dynamic vapor absorption and desorption isotherms of eprosartan mesylate, EPR, EPR:NIC (1:1) cocrystal and EPR:PHB (1:3) eutectic mixture are shown in **Figure 7**. As can be seen, eprosartan mesylate, EPR, and EPR:PHB (1:3) eutectic mixture exhibit a minimal uptake of water (< 0.32%) over a broad humidity range. At 90 % relative humidity (RH), the absorbed water by eprosartan mesylate, EPR, and EPR:PHB (1:3) eutectic mixture were about 0.248, 0.277 and 0.311%, respectively. Conversely, the EPR:NIC (1:1) cocrystal exhibit significant moisture uptake with increasing percent RH, absorbed 3.19% water at 90% RH. The result suggest that EPR cocrystals are slightly more hygroscopic than eprosartan mesylate, EPR and EPR:PHB (1:3) eutectic mixture. Although, the absorption and desorption profile are reversible suggesting no solid state transformation under experimental conditions.

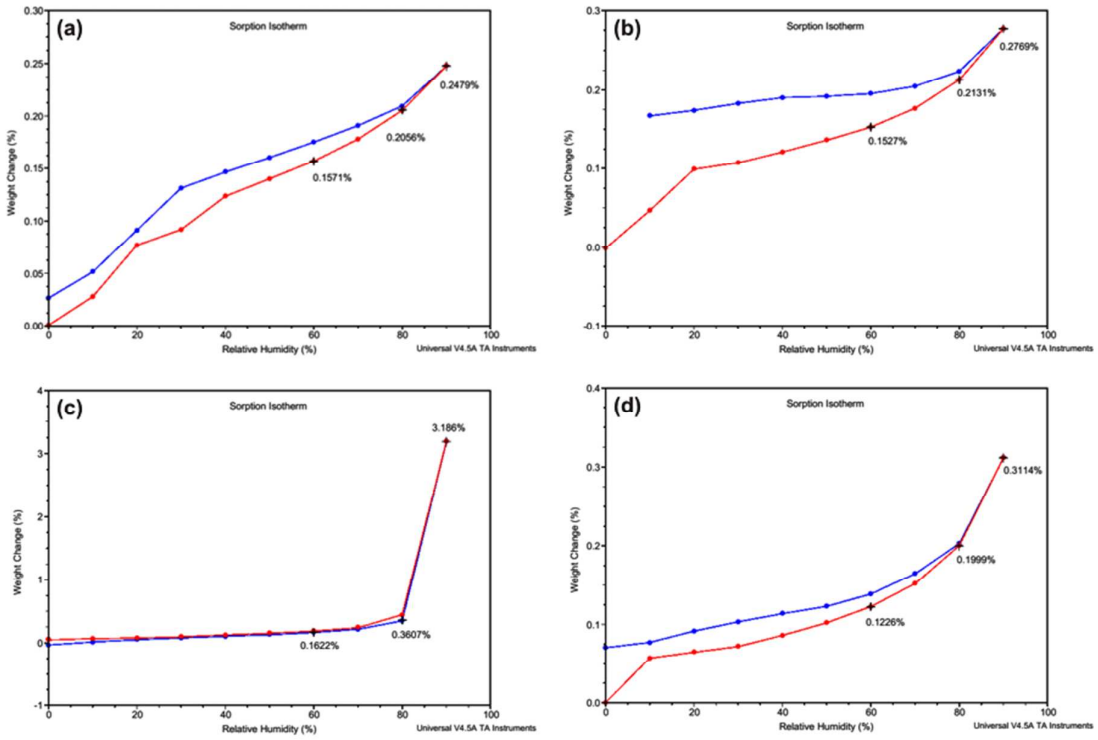

Figure 7. Absorption (red) and desorption (blue) profile of **(a)** eprosartan mesylate, **(b)** EPR, **(c)** EPR:NIC (1:1) cocrystal and **(d)** EPR:PHB (1:3) eutectic mixture.

In vivo pharmacokinetic study

The pharmacokinetic (PK) profiles of EPR, eprosartan mesylate, EPR:NIC (1:1) cocrystal and EPR:PHB (1:3) eutectic mixture after single oral dose administration were determined in SD rats and the results are summarized in **Table 2**. The mean plasma concentration at each time point was used for the PK evaluation.EPR:PHB (1:3) eutectic mixture exhibits a significant ($p < 0.05$) enhancement in oral bioavailability with 2.5, 3.6 and 6.1-fold increase in $AUC_{0\text{-}24h}$ as compared to EPR:NIC (1:1) cocrystal, eprosartan mesylate and EPR, respectively. Similarly, maximum plasma concentration (C_{max}) was increased by 1.5, 1.5 and 3.5-fold as compared to EPR:NIC (1:1) cocrystal, eprosartan mesylate and EPR, respectively. Moreover, the time to reach maxium plasma concentration (t_{max}) was significantly decreased from 6 h to 2 h as compared to EPR **(Figure 8)**. The presence of ultrafine drug crystals in eutectic mixtures may accelerate the dissolution rate and gastrointestinal absorption of EPR and hence, increases the oral bioavailability of EPR[50]. EPR:NIC (1:1) also showed a 1.4 and 2.4-fold increase in $AUC_{0\text{-}24h}$ when compared with eprosartan mesylate and EPR, respectively. This could be attributable primary to the slower elimination rate constant (λ_z). Conversely, there was no significant difference between the C_{max} of EPR:NIC corystal and eprosartan mesylate. Compared to EPR, eprosartan mesylate is more bioavailable with 1.7 and 2.3-fold increase in $AUC_{0\text{-}24h}$ and C_{max}. This increased bioavailability in salt form is attributable to the increase in dissolution rate at all pH as compared with free acid EPR.

Table 2 Pharmacokinetic parameters of EPR, eprosartan mesylate, EPR:NIC (1:1) cocrystal and EPR:PHB (1:3) eutectic mixture after single oral dose administration of 40 mg/kg body weight to Sprague-Dawley rats.

Parameters	EPR	Eprosartan mesylate	EPR:NIC (1:1) cocrystal	EPR:PHB (1:3) eutectic mixture
C_{max} (μg/mL)	9.00 ± 3.36	20.91 ± 5.14[a]	21.03 ± 2.89[a]	31.33 ± 4.09[b¶‡]
$AUC_{0\text{-}24\ h}$ (μg h/mL)	58.50 ± 8.01	98.97 ± 9.04[b]	139.97 ± 11.18[b]	358.64 ± 22.17[c$*]
t_{max} (h)	6	2	4	2
λ_z (h^{-1})	0.071 ± 0.002	0.082 ± 0.001[a]	0.050 ± 0.011[a]	0.047 ± 0.007[a¶]
MRT (h)	13.63 ± 2.09	7.89 ± 1.64[a]	20.31 ± 2.72[b]	20.49 ± 5.70[b$]

All values are mean ± S.D (n = 4/group/time point)

[a]Implies $p < 0.01$, [b]Implies $p < 0.001$, [c]Implies $p < 0.0001$ as compared to EPR.

[¶]Implies $p < 0.01$, [$]Implies $p < 0.0001$ as compared to eprosartan mesylate.

‡Implies $p < 0.01$, *Implies $p < 0.001$ as compared to EPR:NIC (1:1) cocrystal.

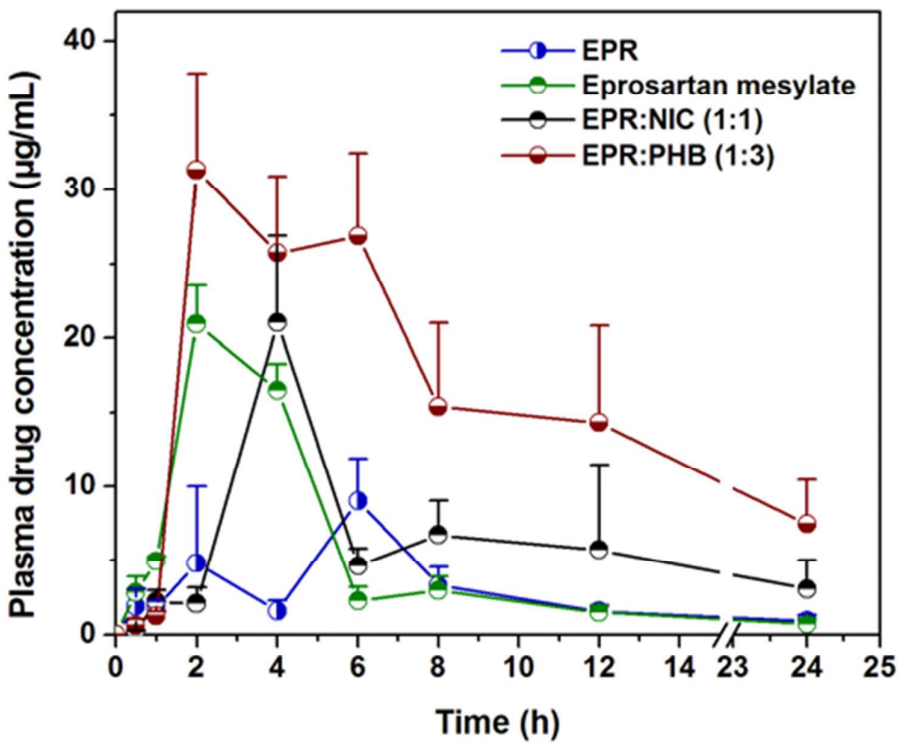

Figure 8. Pharmacokinetic profile of eprosartan mesylate, EPR, EPR:NIC (1:1) cocrystal and EPR:PHB (1:3) eutectic mixture after single oral dose equivalent to 40 mg/kg body weight of eprosartan in SD rats.

Conclusion

Recently, cocrystals are being accepted as an alternative to amorphous solid dispersion in the pharmaceutical industry owing to its superior physicochemical properties. In the present

study, we have reported three cocrystals and four eutectic mixtures of EPR with NIC and PHB, respectively of which EPR:NIC (1:1) cocrystal and EPR:PHB (1:3) eutectic mixture can be of pharmaceutical interest. Initially, all preparations were thoroughly characterized by DSC and PXRD for possible cocrystal/eutectic mixture formation. Properties such as pH dependent solubility, dissolution rate and hygroscopicity of cocrystals/eutectics were measured and compared with eprosartan mesylate and EPR. Eutectic mixtures with PHB are more soluble and stable than cocrystals in all pH conditions. In contrast, cocrystals are less soluble, but dissolved rapidly before transfer to original EPR. This initial boost in dissolution rate could be attributable to the formation of ultrafine particles. In addition, cocrystals are more hygroscopic than eutectics, eprosartan mesylate salt and EPR. A significant increase in oral bioavailability is possible with cocrystal and eutectics, even when cocrystal transformation is suspected based on *in vitro* studies.

Associated content

Supporting Information: ESI-Mass spectra, DSC thermograms, PXRD patterns, ORTEP view of an asymmetric unit of EPR, the basic building block of the EPR crystal, the crystallographic unit cell arrangement of EPR solvate, the corrugated projection of EPR, crystallographic information and hydrogen bonding parameters of EPR crystals. This information is available free of charge via the internet at http://pubs.acs.org/.

Declarations

The Authors declare that they have no conflicts of interest to disclose.

Acknowledgement

We thanks Glenmark Pharmaceuticals Ltd. (Mumbai, India) for providing eprosartan

mesylate as a gift sample. We are also thankful to Prof. Arvind K. Bansal, Department of Pharmaceutics, NIPER, S.A.S Nagar for providing DSC facility. We thanks Director,NIPER, S.A.S Nagar for providing financial support and facilities. The use of X-ray facility at Indian Institute of Science Education and Research (IISER) Mohali is gratefully acknowledged.

References

1. Lukyanov, A. N.; Torchilin, V. P. *Adv. Drug Deliv. Rev.* **2004**, *56*, 1273-1289.
2. O'Donnell, K. P.; Williams III, R. O. In *Formulating poorly water soluble drugs*, AAPS advances in the pharmaceutical sciences Series 3; Williams III, R. O., Watts, A. B., Miller, D. A., Eds.; Springer Science & Business Media: New York, **2012**; Chapter 2, pp 27-93.
3. Frick, A.; Möller, H.; Wirbitzki, E. *Eur. J. Pharm. Biopharm.* **1998**, *46*, 305-311.
4. Serajuddin, A. T. *Adv. Drug Deliv. Rev.* **2007**, *59*, 603-616.
5. Cheng, Y.; Xu, W.; Chen, Z.; Wang, Z.; Huang, D. *J. Supercrit. Fluids.* **2016**, *115*, 10-16.
6. Ahuja, B. K.; Jena, S. K.; Paidi, S. K.; Bagri, S.; Suresh, S. *Int. J. Pharm.* **2015**, *478*, 540-552.
7. Agrawal, A. G.; Kumar, A.; Gide, P. S. *Colloids Surf., B* **2015**,*126*, 553-560.
8. Paidi, S. K.; Jena, S. K.; Ahuja, B. K.; Devasari, N.; Suresh, S. *J. Pharm. Pharmacol.* **2015**,*67*, 616-629.
9. Thipparaboina, R.; Kumar, D.; Mittapalli, S.; Balasubramanian, S.; Nangia, A.; Shastri, N. R. *Cryst. Growth Des.* **2015**,*15*, 5816-5826.
10. Jena, S. K.; Singh, C.; Dora, C. P.; Suresh, S. *Int. J. Pharm.* **2014**, *473*, 1-9.
11. Kawabata, Y.; Wada, K.; Nakatani, M.; Yamada, S.; Onoue, S.*Int. J. Pharm.* **2011**,*420*, 1-10.
12. Trask, A. V.; Motherwell, W. S.; Jones, W. *Int. J. Pharm.* **2006**, *320*, 114-123.
13. Weyna, D. R.; Cheney, M. L.; Shan, N.; Hanna, M.; Zaworotko, M. J.; Sava, V.; Song, S.; Sanchez-Ramos, J. R. *Mol. Pharm.* **2012**,*9*, 2094-2102.
14. Eddleston, M. D.; Arhangelskis, M.; Fabian, L.; Tizzard, G. J.; Coles, S. J.; Jones, W. *Cryst. Growth Des.* **2015**,*16*, 51-58.
15. Chadha, R.; Rani, D.; Goyal, P. *CrystEngComm* **2016**, *18*, 2275-2283.
16. Braga, D.; Grepioni, F.; Lampronti, G. I.; Maini, L.; Turrina, A. *Cryst. Growth Des.* **2011**,*11*, 5621-5627.
17. Fernandes, J. A.; Liu, B.; Tomé, J. P.; Cunha-Silva, L.; Almeida Paz, F. A. *Acta Crystallogr.* **2015**, *E71*, 840-843.
18. Politzer, P.; Murray, J. S. *Cryst. Growth Des.* **2015**,*15*, 3767-3774.

19. Cherukuvada, S. *J. Chem. Sci.* **2016**,*128*, 487-499.
20. Desiraju, G. R. *Angew. Chem. Int. Ed.* **2007**,*46*, 8342-8356.
21. Ram, C. V. S.; Rudmann, M. A. *Expert Rev. Cardiovasc. Ther.* **2007**,*5*, 1003-1011.
22. Crasto, A.; Naik, S.; Joshi, N.; Khan, M. *U.S. Patent 20080014263 A1,* Jan 17, **2008**.
23. Chapelsky, M. C.; Martin, D. E.; Tenero, D. M.; Ilson, B. E.; Boike, S. C.; Etheredge, R.; Jorkasky, D. K. *J. Clin. Pharmacol.* **1998**, *38*, 34-39.
24. Borker, S.; Pawar, A. *ASEM.* **2013**,*5*, 1297-1304.
25. Venkatesh, G.*U.S. patent 20030022928 A1*, Jan 30, **2003**.
26. Bhandaru, J. S.; Malothu, N.; Akkinepally, R. R. *Cryst. Growth Des.* **2015**,*15*, 1173-1179.
27. Tenero, D.; Martin, D.; Ilson, B.; Jushchyshyn, J.; Boike, S.; Lundberg, D.; Zariffa, N.; Boyle, D.; Jorkasky, D. *Biopharm Drug Dispos.* **1998**, *19*, 351-356.
28. Link, P. A.; van der Hulst, M. M.; Bielenberg, G. W.; van den Akker, C. R. *WO Patent 2010003996 A1,* Jan 14, **2010**.
29. *APEX2*, *SADABS and SAINT*; Bruker AXS inc: Madison, WI, U.S.A, **2008**.
30. Sheldrick, G. M.; *Acta Cryst.* **2008***, A64,* 112-122.
31. Macrae, C. F.; Bruno, I. J.; Chisholm, J. A.; Edgington, P. R.; McCabe, P.; Pidcock, E.; Rodriguez-Monge, L.; Taylor, R.; Streek, J. V.; Wood, P. A. *J. Appl. Cryst.* **2008**, *41*, 466-470.
32. Spek, A. L. PLATON, Version 1.62.*University of Utrecht* **1999**.
33. Lin, H. L.; Wu, T. K.; Lin, S. Y. *Thermochim. Acta* **2014**,*575*, 313-321.
34. Jena, S. K.; Sangamwar, A. T. *Carbohyd. Polym.* **2016**, *151*, 1162-1174.
35. Murdande, S. B.; Pikal, M. J.; Shanker, R. M.; Bogner, R. H. *Pharm. Dev. Technol.* **2011**, *16*, 187-200.
36. Zhang, G. G.; Law, D.; Schmitt, E. A.; Qiu, Y. *Adv. Drug Deliv. Rev.* **2004**, *56*, 371-390.
37. Lu, E.; Rodríguez-Hornedo, N.; Suryanarayanan, R.*CrystEngComm* **2008**, *10*, 665-668.
38. Yamashita, H.; Hirakura, Y.; Yuda, M.; Teramura, T.; Terada, K. *Pharm. Res.* **2013**,*30*, 70-80.
39. Goud, N. R.; Suresh, K.; Sanphui, P.; Nangia, A. *Int. J. Pharm.* **2012**, *439*, 63-72.
40. Manin, A. N.; Voronin, A. P.; Drozd, K. V.; Manin, N. G.; Bauer-Brandl, A.; Perlovich, G. L. *Eur. J. Pharm. Sci.* **2014**,*65*, 56-64.
41. Cherukuvada, S.; Nangia, A. *Chem. Commun.* **2014**,*50*, 906-923.
42. Goldberg, A. H.; Gibaldi, M.; Kanig, J. L. *J. Pharm. Sci.* **1966**,*55*, 482-487.
43. Sinha, S.; Ali, M.; Baboota, S.; Ahuja, A.; Kumar, A.; Ali, J. *AAPS PharmSciTech* **2010**,*11*, 518-527.
44. Hathwar, V. R.; Pal, R.; Guru Row, T. N. *Cryst. Growth Des.* **2010**,*10*, 3306-3310.
45. Huddleston, J. G.; Willauer, H. D.; Swatloski, R. P.; Visser, A. E.; Rogers, R. D. *Chem. Commun.* **1998***,* 16, 1765-1766.
46. http://www.drugbank.ca/drugs/DB00876 (Accessed September 7, **2015**).

47. Keramatnia, F.; Shayanfar, A.; Jouyban, A. *J. Pharm. Sci.* **2015**,*104*, 2559-2565.
48. Qiao, N.; Li, M.; Schlindwein, W.; Malek, N.; Davies, A.; Trappitt, G. *Int. J. Pharm.* **2011**, *419*, 1-11.
49. Good, D. J.; Rodríguez-Hornedo, N. *Cryst. Growth Des.* **2010**,*10*, 1028-1032.
50. Goldberg, A. H.; Gibaldi, M.; Kanig, J. L. *J. Pharm. Sci.* **1966***, 55*, 482-48

For Table of Contents Use Only

Multicomponent pharmaceutical adducts of α-eprosartan: physicochemical properties and pharmacokinetics study.

Sawani G. Khare[1¶], Sunil K. Jena[2¶], Abhay T. Sangamwar[3*], Sadhika Khullar[4], Sanjay K. Mandal[4]

[1]Department of Pharmacoinformatics, [2]Department of Pharmaceutical Technology (Formulations), [3]Department of Pharmaceutics, National Institute of Pharmaceutical Education and Research, Sector-67, S.A.S Nagar-160062, Punjab, India.

[4]Department of Chemical Sciences, Indian Institute of Science Education and Research Mohali, Sector-81, S.A.S. Nagar -140306, Punjab, India

[¶]These authors contributed equally to this work.

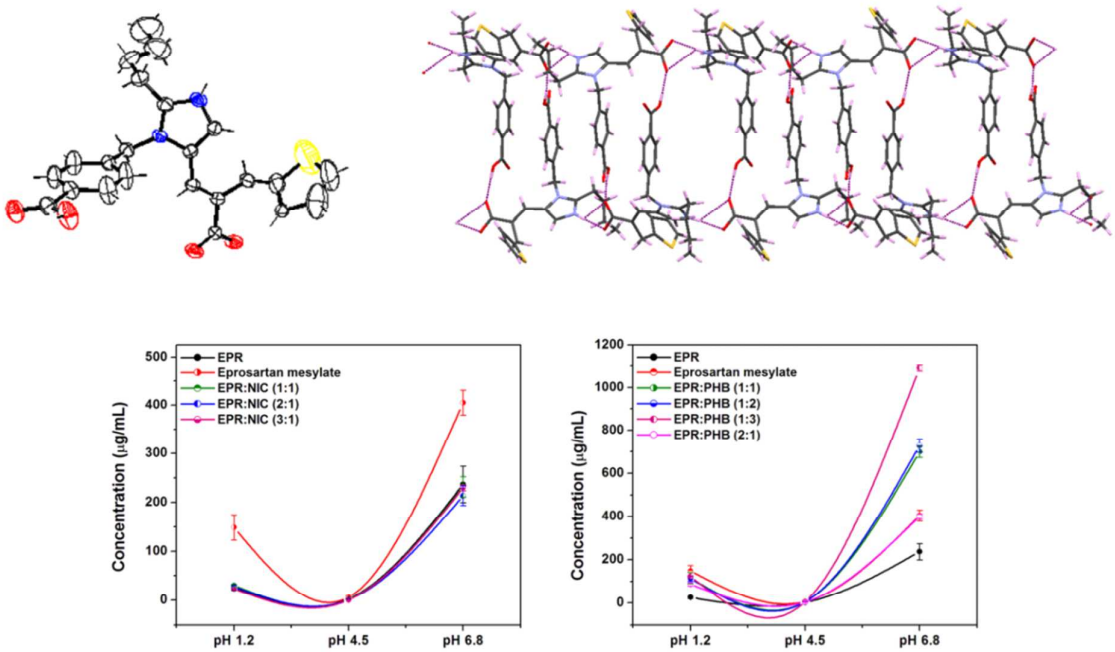

Synposis: Two screened coformers, nicotinamide (NIC) and p-hydroxybenzoic acid (PHB) are used in this work to prepare pharmaceutical adducts of α-eprosartan (EPR). The generated cocrystals and eutectics are characterised and employed towards the goal of improving bioavailability of EPR. The EPR:PHB eutectics proved better in improving apparent solubility, dissolution rate and bioavailability of EPR.